37. Bache R, Cobb F. Effect of maximal coronary vasodilation on transmural myocardial perfusion during tachycardia in the awake dog. *Circ Res* 1977;41:648–653.
38. Hoffman E. Maximal coronary flow and the concept of coronary vascular reserve. *Circulation* 1984;70:153–165.
39. Ohtsuka S, Kakihana M, Sugishita Y, Ito I. Effects of the rise in aortic blood pressure on coronary flow reserve in dogs. *Jpn Heart J* 1987;28:403–412.
40. McGinn A, White C, Wilson R. Interstudy variability of coronary flow reserve: Influence of heart rate, arterial pressure and ventricular preload. *Circulation* 1990;81: 1319–1330.
41. Klocke F, Ellis A, Canty J, Jr. Interpretation of changes in coronary flow that accompany pharmacologic interventions. *Circulation* 1987;75(suppl V):34–38.

Comparison of Myocardial Uptake of Fluorine-18-Fluorodeoxyglucose Imaged with PET and SPECT in Dyssynergic Myocardium

Jeroen J. Bax, Frans C. Visser, Paul K. Blanksma, Magreet A. Veening, Eng S. Tan, Antoon T.M. Willemsen, Arthur van Lingen, Gerrit J.J. Teule, Willem Vaalburg, Kong I. Lie and Cees A. Visser
Departments of Cardiology and Nuclear Medicine, Free University Hospital Amsterdam; and the PET Center of the Groningen University Hospital, Groningen, The Netherlands

PET with ^{18}F-fluorodeoxyglucose (FDG) can detect viable myocardium and predict functional recovery after revascularization. The use of PET for clinical routine, however, is limited. Recently, imaging FDG with SPECT was proposed. The aim of this study was to compare the diagnostic value of FDG-PET and FDG-SPECT in the detection of viable myocardium in segments with abnormal wall motion. **Methods:** Twenty patients with previous myocardial infarction were studied. All underwent FDG-PET and FDG-SPECT during hyperinsulinemic glucose clamping. Regional perfusion was assessed with ^{13}N-ammonia PET and early resting ^{201}Tl- SPECT. Regional wall motion was assessed with two-dimensional echocardiography. The agreement between FDG/^{13}N-ammonia PET and FDG/^{201}Tl SPECT to detect viability in dyssynergic myocardium was 76%. On a patient basis, PET and SPECT yielded comparable results in 17 of 20 patients. In a subgroup of patients with LVEF ≤ 35% (n = 12), all PET and SPECT viability data were identical. **Conclusion:** This study shows a good correlation between the detection of viability in dyssynergic myocardium with FDG/^{13}N-ammonia PET and FDG/^{201}Tl SPECT, both on a segmental and patient basis.

Key Words: PET; fluorine-18-fluorodeoxyglucose; SPECT; myocardial viability

J Nucl Med 1996; 37:1631–1636

Dyssynergic but viable myocardium can be detected with PET using ^{18}F-fluorodeoxyglucose (FDG) (*1–4*). PET centers, however, are not widely available to meet the clinical demand for viability studies with FDG. Several institutions have recently studied the feasibility of imaging myocardial FDG uptake with SPECT (*5–10*). Two recent reports described good agreement between myocardial FDG uptake assessed with PET and SPECT (*8,10*). Moreover, we have previously shown that FDG-SPECT can predict improvement of regional contractile function after revascularization (*11*).

In this study, we compared the diagnostic value of FDG-PET and FDG-SPECT in the detection of residual viability in dyssynergic myocardium (assessed by echocardiography). For comparison, not only was FDG uptake considered, but also its uptake relative to a flow tracer (^{13}N-ammonia in the PET study and ^{201}Tl in the SPECT study). Quantitative analysis techniques were applied to the PET and SPECT data, to minimize observer bias.

Received Sept. 27, 1995; revision accepted Jan. 24, 1996.
For correspondence or reprints contact: Jeroen J. Bax, MD, Department of Cardiology, University Hospital Leiden, Rijnsburgerweg 10, 2333 AA Leiden, The Netherlands.

MATERIALS AND METHODS

Patients and Study Protocol

Twenty patients (4 women, 16 men; mean age 64 ± 8 yr) with previous infarction were included. Six patients had a non-Q wave infarction, and 14 had a Q wave on the ECG (6 inferior, 7 anterior and 1 both anterior and inferior). The mean time interval of infarction to the study was 42 ± 57 mo. All patients who underwent catheterization, had significant coronary artery disease on angiography (>50% reduction in luminal diameter of at least one major epicardial coronary artery (*25*)). Ten had three-vessel disease, five had two-vessel disease and three had single-vessel disease. They had a mean left ventricular ejection fraction (LVEF) of 39% ± 16% (12 patients had LVEF ≤ 35%). Four patients had diabetes mellitus type II and were well regulated on oral hypoglycemics. All patients underwent PET and SPECT studies to evaluate myocardial viability in dyssynergic myocardium. The mean time interval between the PET and SPECT studies was 34 ± 20 days (range 6–62 days). The investigators analyzing the PET, SPECT or echocardiographic data were unaware of the results of the other modalities. Cardiac catheterization was performed in 18 patients within 3 mo of the scintigraphic studies.

None of the patients experienced unstable angina pectoris or myocardial infarction during the study period. Cardiac medication remained unchanged during the entire study period. All patients gave informed consent to the study protocol that was approved by the Ethical Committee of the Free University Hospital Amsterdam.

Two-Dimensional Echocardiography

Echocardiography was performed within 2 wk of the scintigraphic studies. Four standard views of the left ventricle were obtained: parasternal long- and short-axis views and apical two- and four-chamber views. The images were reviewed off-line and consensus was achieved by two observers unaware of the PET/SPECT data. For comparison with the PET/SPECT data (Fig. 1) the left ventricle was divided into 13 segments (*12*). Both wall motion and thickening were analyzed. Each segment was assigned a wall motion score (WMS) of 0 to 3: normal = 0, hypokinetic = 1, akinetic = 2 and dyskinetic = 3.

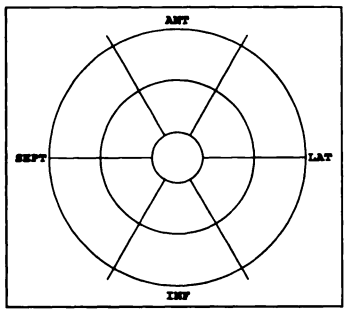

FIGURE 1. PET and SPECT polar maps were divided into 13 segments: 1 apical segment (center), 6 segments representing the distal myocardium and 6 segments representing the basal myocardium (anterior, lateral, inferior and septal).

Evaluation of Regional Perfusion with Thallium-201 SPECT

Thallium SPECT was performed within 15 min after tracer injection (111 MBq) under resting conditions to assess regional perfusion. Previously, Melin et al. (*13*) showed that the initial myocardial uptake of thallium is proportional to regional perfusion. Thallium images were acquired with a large field of view rotating dual-head gamma camera equipped with low-energy high-resolution (LEHR) collimators. The dual-head gamma camera system was rotated over 360°, collecting 64 views for 30 sec each. From the raw scintigraphic data 6-mm thick (1 pixel) transaxial slices were reconstructed by filtered back projection using a Hanning filter (f_c = 0.63 cycle.cm^{-1}). Slices were not corrected for attenuation. Further reconstruction yielded short-axis slices perpendicular to the heart axis.

FDG-SPECT during Hyperinsulinemic Euglycemic Clamping

After the ^{201}Tl SPECT study, the hyperinsulinemic euglycemic clamp was started as described previously (*14*). After 60 min of clamping, 185 MBq FDG were injected and 45 min were allowed for tracer clearance and myocardial trapping (*15*). FDG was produced according to the method of Stöcklin et al. (*16*).

Data acquisition was performed with the same camera system as described for ^{201}Tl, which was now equipped with 511 keV collimators (*17*). The in-plane resolution of the system was 14 mm FWHM in 10 cm water for FDG. Data reconstruction was identical to that for ^{201}Tl data.

SPECT Image Analysis

Circumferential count profiles (60 sectors, highest pixel activity/sector) were generated from the ^{201}Tl and FDG short-axis slices. Twenty slices (with each 60 sectors) for each study were acquired by linear interpolation of the available slices and presented in a polar map. The polar maps were divided into 13 segments for comparison with PET data and echocardiography (Fig. 1).

An area of normal perfusion was chosen on the ^{201}Tl polar map, based on the highest ^{201}Tl uptake and normal wall motion on the echocardiogram. The activity of this area was normalized to the mean activity of the same area of a normal database [obtained in normal individuals (*6*)]. All other polar map data were adjusted correspondingly. The region of normal perfusion was projected on the FDG polar map and the same normalization procedure was followed. For this purpose, a database of FDG uptake in normals was used (*6*). The ^{201}Tl and FDG activities were expressed as percentage of the corresponding normal reference values. A particular segment was considered as a perfusion defect when > 50% of the pixels in that segment had ^{201}Tl activity < 2 s.d. below the normal reference value on the ^{201}Tl polar map.

Definition of Myocardial Viability on FDG/Thallium SPECT

For the detection of viable/nonviable tissue, we only considered the segments with abnormal wall motion on echo. A segment was considered viable if the perfusion was normal, or if increased FDG uptake was ≥ 7% relative to the ^{201}Tl uptake in the perfusion defect (*18*). The cutoff level of 7% increased FDG uptake in perfusion defects has been established using ROC analysis on the level of increased FDG uptake in perfusion defects, in 44 patients undergoing revascularization (*18*). Segments with a perfusion defect and increased FDG uptake < 7% relative to the ^{201}Tl uptake were considered nonviable.

Evaluation of Perfusion with Nitrogen-13-Ammonia

Myocardial perfusion was evaluated with dynamic ^{13}N-ammonia imaging as described previously (*19,20*). The patients were positioned in a 951 Siemens ECAT positron camera, imaging 31 planes simultaneously over 10.8 cm and equipped with a ^{68}Ge/ ^{68}Ga retractable ring source for transmission scans. The spatial resolution of the system was 6 mm FWHM. Images were corrected for attenuation by using coefficients measured by a transmission scan. Emission scans were obtained immediately after an injection of 370 MBq ^{13}N-ammonia. Dynamic imaging was continued for 15 min.

Evaluation of Glucose Uptake with FDG

The FDG-PET study was performed during the hyperinsulinemic glucose clamping (*14*). After administration of 185 MBq FDG, dynamic imaging was started and continued for 55 min.

PET Image Analysis

The PET image analysis was performed as described previously, using parametric polar maps (*19,20*). The available ^{13}N-ammonia and FDG data were reoriented into 10 short-axis images. The myocardium in each short-axis slice was divided into 48 sectors of 7.5° each, yielding a total of 480 sectors. In all sectors, time-activity curves were generated. The left ventricular blood pool was defined in three basal slices; the average was used to obtain a single blood-pool time-activity curve. Absolute segmental myocardial perfusion was determined using a curve fit method over a period of 120 sec (*21*). To correct for perfusion-mediated extraction, the following correction was applied as described by Schelbert et al. (*22*): $E = E_0 \times (1 - 0.607 \times e^{-1.25/flow})$. Sectorial glucose uptake was calculated with Patlak analysis of blood-pool and myocardial time activity curves (*23,24*). The slope of the Patlak curve was calculated from data acquired 5 min after tracer injection.

From the these data, ^{13}N-ammonia and FDG parametric polar maps were constructed. The 480 sectors of the PET data were grouped into 13 segments (Fig. 1).

Definition of Myocardial Viability on FDG/Nitrogen-13-Ammonia PET

To assess myocardial viability, a ratio map (13 segments) was constructed from the FDG and perfusion studies by calculating the ratio of glucose uptake and perfusion (*19*). In a previous study, 95% confidence intervals of the normal FDG/perfusion ratio (from mean − 2 s.d. to mean + 2 s.d.) were obtained in normal volunteers (*19*). A segment was defined as viable when more than 50% of the segment had a FDG/perfusion ratio within the 95% confidence interval or when more than 50% of the segment had a ratio exceeding the 95% confidence interval (a mismatch pattern). To quantify nonviable myocardium, the ratio FDG/^{13}N-ammonia polar map was normalized for flow (glucose uptake × Fi/Fmean (Fi = segmental flow; Fmean = mean flow) (*19*). A segment was defined nonviable when more than 50% of the segment had a ratio below the 95% confidence interval (match pattern).

FDG Uptake Analysis

The PET data were compared with the normalized segmental FDG activities on SPECT, to exclude the influence of ^{201}Tl on the SPECT data. In addition, to compare the FDG-SPECT activities directly to the FDG-PET activities, the FDG-PET and SPECT segmental activities were expressed as percentage of maximum uptake.

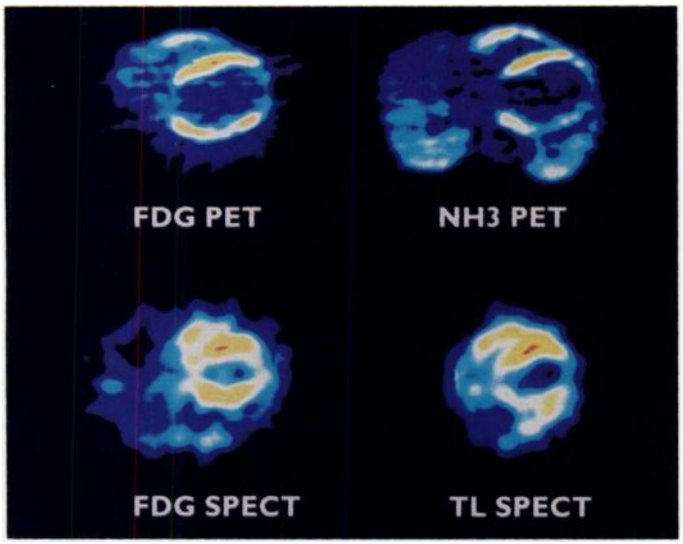

FIGURE 2. Corresponding transaxial slices of a patient with a matching defect in the anteroapical region (decreased perfusion and decreased FDG uptake) and a mismatch in the infero-lateral region (decreased perfusion with preserved FDG uptake). Although the resolution of the SPECT images is inferior to the PET images, the clinical relevant information can be derived from both studies.

Statistical Analysis

All data are expressed as mean ± s.d. Mean values were compared using an unpaired Student's t-test. Linear regression analysis was used to analyze the relation between normalized FDG-SPECT and FDG-PET activities. Chi-square analysis was used to compare distributions between groups. A P-value ≤ 0.05 was considered significant.

RESULTS

Image Analysis

The image quality of the FDG-SPECT images are shown in Figure 2, which depict transaxial FDG-PET, ^{13}N-ammonia PET, FDG-SPECT and ^{201}Tl SPECT slices in a patient. Additionally, good image quality of cardiac FDG studies can be obtained in patients with diabetes when the hyperinsulinemic glucose clamp is used (*26,27*).

Regional Wall Motion Compared with Scintigraphic Findings

Of the 260 segments evaluated, 123 (47%) had normal wall motion and 137 (53%) had abnormal wall motion, with a mean of 7 ± 4 dyssynergic segments per patient. In particular, 1 segment showed dyskinesia, 81 showed akinesia and 55 revealed hypokinesia.

In the 137 dyssynergic segments, 67 (49%) were nonviable according to PET; 52 (78%) segments were also nonviable on SPECT. PET characterized 70 (51%) segments as viable, whereas SPECT showed viability in 52 (74%) of these segments. The concordance in the dyssynergic segments was 76% (Fig. 3). The dyssynergic segments were divided into akinetic or dyskinetic (n = 82) segments and hypokinetic (n = 55) segments. In the a-/dyskinetic segments, 52 (63%) segments were nonviable on PET, with 41 (79%) segments also nonviable on SPECT. Thirty (37%) segments were viable on PET, and SPECT showed viability in 20 (67%) (concordance 74%). In the 55 hypokinetic segments, 15 (27%) were necrotic by PET, with 11 (73%) also necrotic by SPECT. Forty (73%) segments were viable on PET, of which 32 (80%) were viable on SPECT (concordance 89%).

Location of Discordant Segments

Table 1 shows the distribution of concordant and discordant segments in the dyssynergic segments according to the location. The discordant segments were evenly distributed over the PET-viable/SPECT-nonviable group and the PET-nonviable/SPECT-viable group (ns). The highest number of discordant segments were observed in the lateral wall ($p < 0.05$ compared with all other locations).

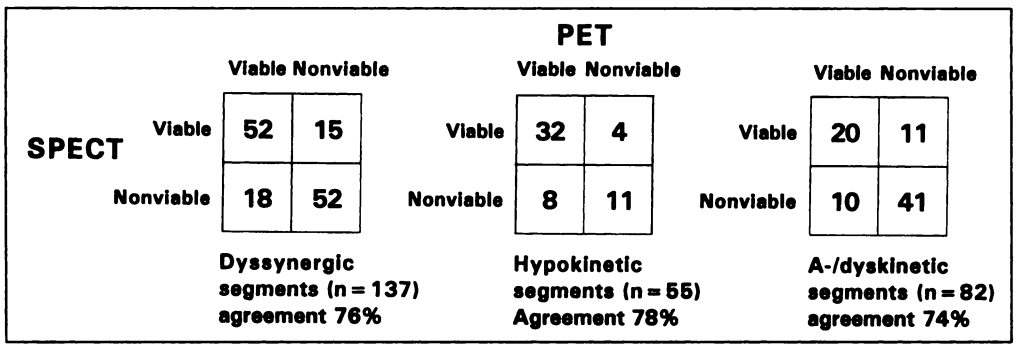

FIGURE 3. Comparison of PET and SPECT data in all dyssynergic segments (n = 137).

TABLE 1
Frequency of Concordant and Discordant Segments in Regions with Dyssynergy (n = 137)*

Dyssynergic segments (n = 137)	PET viable SPECT viable	PET viable SPECT nonviable	PET nonviable SPECT viable	PET nonviable SPECT nonviable
Apex	1 (7%)	0 (–)	3 (21%)	10 (71%)
Lat	15 (41%)	8 (22%)†	7 (19%)†	7 (19%)
Inf	20 (63%)	3 (9%)	0 (–)	9 (28%)
Sept	13 (36%)	3 (8%)	4 (11%)	16 (44%)
Ant	3 (16%)	4 (22%)	1 (6%)	10 (56%)

*Numbers are divided according to the different myocardial regions.
†Significantly more discordancies between PET and SPECT were located in the lateral wall as compared to the other regions ($p < 0.05$).
Ant = anterior; inf = inferior; lat = lateral; sept = septal.

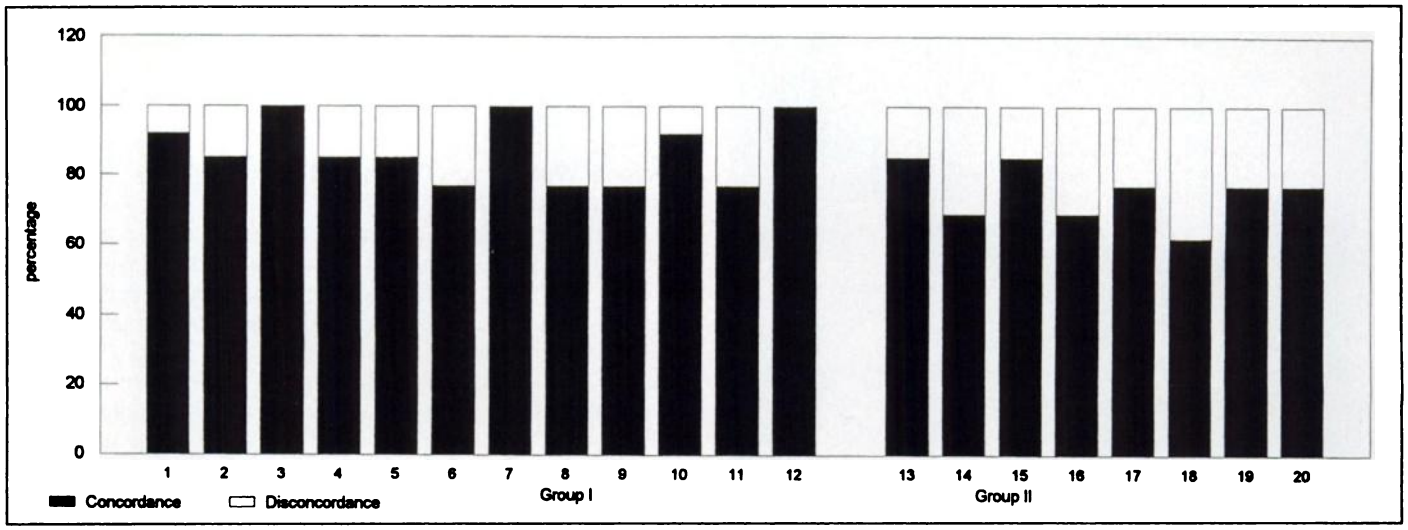

FIGURE 4. Bar graph demonstrating the agreement of PET and SPECT data on a patient basis. The patients are grouped according to LVEF (left: patients (n = 12, Group I) with LVEF ≤ 35%, right: patients (n = 8) with LVEF > 35%, Group II). In 85% of the patients an agreement of more than 70% of all segments was found.

Comparison between PET and SPECT Findings

PET and SPECT data were also compared in individual patients; the percentage of agreement in each patient is presented in Figure 4. In three patients, the PET and SPECT data showed complete agreement; in an additional 14 patients, the agreement was > 70% between PET and SPECT data. In the previous three patients, the agreement was < 70%. Importantly, these patients all had a LVEF > 35%; all patients with a LVEF ≤ 35% showed an agreement > 70%.

PET Classification Compared with FDG Activity on SPECT

In Table 2 and Figure 5 the normalized FDG-SPECT activity was compared with the PET results. All dyssynergic segments with normalized FDG uptake < 40% on SPECT were nonviable by PET, whereas in the segments with FDG uptake > 90% only 8% of segments were nonviable by PET. In the PET viable segments, the normalized FDG-SPECT activity was significantly higher than in the PET nonviable segments (85.7%±16.0% compared with 64.0% ± 15.5%, $p < 0.01$). When a cutoff-level of 70% normalized FDG uptake on SPECT was used to detect viable myocardium (*28*), FDG-SPECT correctly detected 58 (73%) of 79 PET viable segments and correctly depicted 47 (81%) of 58 PET nonviable segments. Thus, when only normalized FDG uptake on SPECT was considered, the agreement between both techniques was 77%.

Finally, comparison of the normalized segmental FDG-PET and FDG-SPECT activities showed a linear relation: $y = 1.0 \times x - 11.1$, $r = 0.79$, $p < 0.001$ (Fig. 6).

TABLE 2
Distribution of Viable/Nonviable Segments (assessed by PET) According to Normalized FDG Activity on SPECT in Dyssynergic Segments

FDG-SPECT activity (%)	Number of segments	PET viable	PET nonviable
<40	5	-	5 (100%)
41–50	9	2 (22%)	7 (78%)
51–60	21	5 (24%)	16 (76%)
61–70	23	5 (22%)	18 (78%)
71–80	23	14 (61%)	9 (39%)
81–90	19	10 (53%)	9 (47%)
>90	37	34 (92%)	3 (8%)

DISCUSSION

This study showed good agreement between FDG/^{201}Tl SPECT and FDG/^{13}N-ammonia PET to assess myocardial viability segmentally and in individual patients. These data provide further evidence that FDG/^{201}Tl SPECT can be used to detectviable myocardium in patients with coronary artery disease.

In the present study, the PET images had superior image quality compared to the SPECT images, due to the superior resolution of PET. Nonetheless, comparable clinical information was derived in all patients with a LVEF ≤ 35% (see Fig.

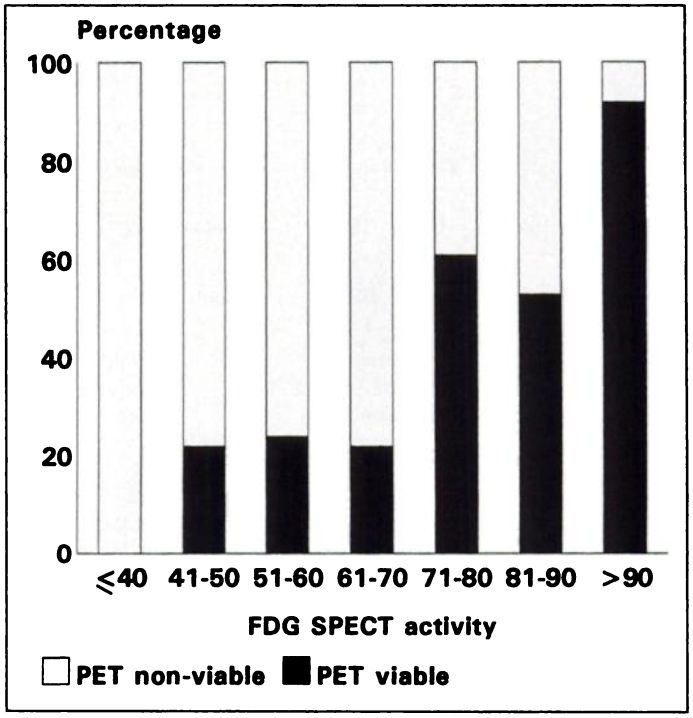

FIGURE 5. Bar graph comparing viability, as assessed by PET, with the normalized FDG activity on SPECT imaging. The frequency of viable myocardium increased from 0% in dyssynergic segments with < 40% FDG uptake on SPECT to 92% in the segments with > 90% FDG uptake; on the contrary, the presence of nonviable tissue decreased from 100% in the segments with FDG- SPECT activity < 40% to 8% in segments with > 90% FDG-SPECT activity.

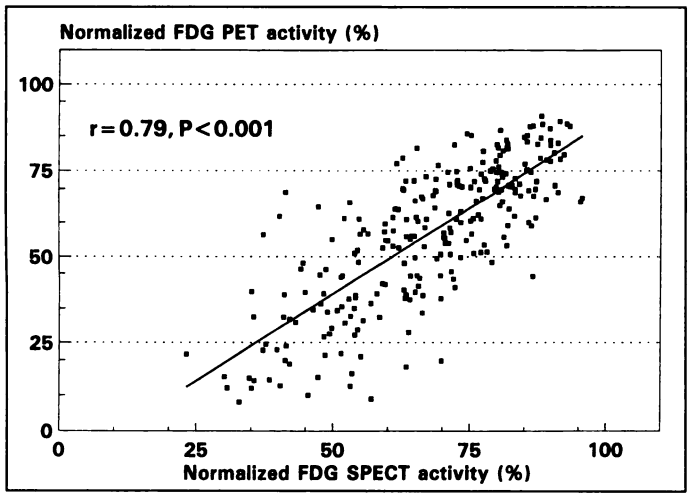

FIGURE 6. Scatter plot showing the relation between normalized FDG-SPECT and FDG-PET activities.

4); in this category of patients, detection of residual viability in regions with dyssynergy is of paramount importance for clinical management. Overall agreement of 76% in dyssynergic segments was found. This finding is in line with recently published data, reporting good agreement between FDG-SPECT and FDG-PET (*8,10*). Further analysis of discordant segments showed that 15 of 33 discordant segments were located in the lateral wall, whereas only three discordant segments were located in the inferior wall and seven in the septal region. Moreover, a similar number of PET-viable/SPECT-nonviable and PET- nonviable/SPECT-viable segments was observed in the inferior and septal regions. Considering the difference in photon energies between ^{18}F and ^{201}Tl, discrepancies between tissue classification by PET and SPECT due to attenuation were expected in the inferior and septal wall. The present data suggest that attenuation does not markedly influence the identification of viable myocardium with the FDG/^{201}Tl SPECT protocol, although the number of patients may be to small to draw definitive conclusions on this topic.

The finding of the relatively high frequency of discordant segments in the lateral wall is surprising. Decreased myocardial wall thickness in the dyssynergic segments may have resulted in loss of count density (partial volume effect) (*29*). The SPECT system will be more affected by this phenomenon because of the lower spatial resolution. Nevertheless, discordant classifications of PET-viable/SPECT-nonviable and PET nonviable/SPECT viable were evenly distributed (Table 1). It is possible that the different quantitative approaches of both techniques might have led to these errors.

Finally, the PET data were compared with the normalized segmental FDG activities on SPECT (Fig. 5, Table 2). This approach excludes the influence of ^{201}Tl in the SPECT protocol. Moreover, several PET studies have used the percentage of FDG uptake as marker of viable myocardium (*28,30–32*). Our results show that the frequency of viable myocardium (as assessed by PET) increased from 0% in segments with < 40% FDG uptake on SPECT to 92% in the segments with > 90% FDG uptake on SPECT. We used a cutoff level of 70% FDG uptake to detect viability as previously described by Altehoefer et al. (*28*). By using this cutoff level, we found an agreement between PET and SPECT of 77%. This cutoff level, however, has not been validated in patients undergoing revascularization.

The direct comparison between normalized FDG-PET and FDG-SPECT activities showed a good correlation (Fig. 6), although there was considerable scatter of the individual data about the regression line. The scatter may be caused by variation between the individual relations.

Methodologic Considerations and Limitations

It should be emphasized that the patients in the present study did not undergo revascularization. Therefore, the comparison of PET and SPECT data with functional outcome was not possible.

We used a quantitative approach for both PET and SPECT to minimize possible observer bias. For the PET approach, we used a ratio of FDG to ^{13}N-ammonia, using absolute perfusion and glucose utilization, displayed in parametric polar maps. The rationale for this approach is twofold. First, this approach takes into account the advantage of PET overall other scintigraphic procedures, i.e., absolute quantification of tracer uptake. Second, utilization of parametric polar maps has been demonstrated to avoid false-positive ^{13}N-ammonia perfusion defects in the postero-lateral region, as frequently observed on static images (*20*).

For the SPECT approach, absolute quantification is not possible. Instead, we have compared FDG uptake with regional perfusion to assess myocardial viability. We have previously demonstrated that this approach can adequately predict functional recovery (*11,18*). Finally, the PET and SPECT studies were performed in two different centers, which have gained experience with different analytical procedures. Nevertheless, despite these different approaches, we found a good agreement between the two techniques. Possibly, the newer SPECT systems may improve sensitivity and resolution and may further improve the agreement between PET and SPECT.

In addition, the time interval between the PET and SPECT study was 34 ± 20 days. Although none of the patients had either unstable angina pectoris or myocardial infarction during the study period, silent reinfarction or progression of severely hibernating tissue to necrosis may have occurred, which may account for some of the discordancies observed.

The segments were compared in a similar polar map format, still some misalignment between segments may have occurred. Although several findings, described earlier, suggest that attenuation of ^{201}Tl in the infero-septal region does not significantly reduce the diagnostic accuracy of the FDG/^{201}Tl SPECT approach, it would be important to perform a similar study using attenuation correction to further address this feature. Finally, Sandler et al. (*33*) have recently reported on the use of dual-isotope ^{99m}Tc-MIBI/FDG-SPECT imaging. This approach may be more cost-effective and less time-consuming than the FDG/^{201}Tl approach as described by our group and other investigators.

CONCLUSION

Our study shows good correlation between detection of myocardial viability with FDG/^{201}Tl SPECT and FDG/^{13}N-ammonia PET segmentally and on a patient basis. The results suggest that FDG/^{201}Tl SPECT may contribute to the detection of myocardial viability. Further clinical studies comparing PET and SPECT with a larger number of patients, who also undergo revascularization, are needed to assess the future role of FDG/^{201}Tl SPECT for clinical routine.

REFERENCES

1. Schwaiger M, Hicks R. The clinical role of metabolic imaging of the heart by positron emission tomography. *J Nucl Med* 1991;32:565–578.
2. Tillisch J, Brunken R, Marshall R, et al. Reversibility of cardiac wall motion abnormalities predicted by positron tomography. *N Engl J Med* 1986;314:884–888.
3. Tamaki N, Yonekura Y, Yamashita K, et al. Positron emission tomography using fluorine-18-fluorodeoxyglucose in evaluation of coronary artery bypass grafting. *Am J Cardiol* 1989;64:860–865.
4. Marwick TH, MacIntyre WJ, Lafont A, Nemec JJ, Salcedo EE. Metabolic responses of

hibernating and infarcted myocardium to revascularization. *Circulation* 1992;85:1347–1353.
5. Bax JJ, Visser FC, van Lingen A, et al. Feasibility of assessing regional myocardial uptake of ^{18}F-fluorodeoxyglucose using single-photon emission computed tomography. *Eur Heart J* 1993;14:1675–1682.
6. Bax JJ, Visser FC, van Lingen A, et al. Relation between myocardial uptake of thallium-201 chloride and fluorine-18-fluorodeoxyglucose imaged with SPECT in normal volunteers. *Eur J Nucl Med* 1995;22:56–60.
7. Bax JJ, Visser FC, van Lingen A, Visser CA, Teule GJJ. Myocardial ^{18}F-fluorodeoxyglucose imaging by single-photon emission computed tomography. *Clin Nucl Med* 1995:20:466–490.
8. Martin WH, Delbeke D, Patton JA, et al. FDG-SPECT: correlation with FDG-PET. *J Nucl Med* 1995;36:988–995.
9. Stoll HP, Hellwig N, Alexander C, Oezbek C, Schieffer H, Oberhausen E. Myocardial metabolic imaging by means of fluorine-18-fluorodeoxyglucose/technetium-99m-sestamibi dual-isotope single-photon emission tomography. *Eur J Nucl Med* 1994;21:1085–1093.
10. Burt RW, Perkins OW, Oppenheim BE, et al. Direct comparison of [^{18}F]FDG-SPECT, [^{18}F]FDG-PET and rest thallium-201 SPECT for the detection of myocardial viability. *J Nucl Med* 1995;36:176–179.
11. Bax JJ, Cornel JH, Visser FC, et al. The role of fluorine-18-fluorodeoxyglucose single-photon emission computed tomography in predicting reversibility of regional wall motion abnormalities after revascularization. In: van der Wall EE, Blanksma PK, Niemeyer MG, Paans AMJ, eds. *Cardiac positron emission tomography.* Dordrecht: Kluwer Academic Publishers; 1995:75–85.
12. Jaarsma W, Visser CA, Eenige van MJ, et al. Prognostic implications of regional hyperkinesia and remote asynergy of noninfarcted myocardium. *Am J Cardiol* 1986;58:394–398.
13. Melin JA, Becker LC. Quantitative relationship between global left ventricular thallium uptake and blood flow: effects of propranolol, ouabain, dipyridamole and coronary artery occlusion. *J Nucl Med* 1986;27:641–652.
14. Knuuti J, Nuutila P, Ruotsalainen U, et al. Euglycemic hyperinsulinemic clamp and oral glucose load in stimulating myocardial glucose utilization during positron emission tomography. *J Nucl Med* 1992;33:1255–1262.
15. Phelps ME, Hoffman EJ, Selin C, et al. Investigation of [^{18}F]2-fluoro-2-deoxyglucose for the measure of myocardial glucose metabolism. *J Nucl Med* 1978;19:1311–1319.
16. Hamacher K, Coenen HH, Stocklin G. Efficient Stereospecific synthesis of no-carrier-added 2-[^{18}F]-fluoro-2-deoxy-D-glucose using aminopolyether supported nucleophilic substitution. *J Nucl Med* 1986;27:235–238.
17. Van Lingen A, Huijgens PC, Visser FC, et al. Performance characteristics of a 511-keV collimator for imaging positron emitters with a standard gamma-camera. *Eur J Nucl Med* 1992;19:315–321.
18. Bax JJ, Cornel JH, Visser FC, et al. Functional recovery after revascularization predicted by quantitative FDG-SPECT [Abstract]. *Eur J Nucl Med* 1995;22:798.
19. Blanksma PK, Willemsen ATM, Meeder JG, et al. Quantitative myocardial mapping of perfusion and metabolism using parametric polar map displays in cardiac PET. *J Nucl Med* 1995;36:153–158.
20. De Jong RM, Blanksma PK, Willemsen ATM, et al. Posterolateral defect of the normal human heart investigated with nitrogen-13-ammonia and dynamic PET. *J Nucl Med* 1995;36:581–585.
21. Bellina CR, Parodi O, Camici P, et al. Simultaneous in vitro and in vivo validation of nitrogen-13-ammonia for the assessment of myocardial blood flow. *J Nucl Med* 1990;31:1335–1343.
22. Schelbert HR, Phelps ME, Huang SC, et al. Nitrogen-13-ammonia as an indicator of myocardial blood flow. *Circulation* 1981;63:1259–1272.
23. Krivokapich J, Huang SC, Phelps ME, et al. Estimation of myocardial metabolic rate for glucose using fluoro-18-deoxyglucose. *Am J Physiol* 1982;12:H884–H895.
24. Ratib O, Phelps ME, Huang SC, et al. Positron emission tomography with deoxyglucose for estimating local myocardial glucose metabolism. *J Nucl Med* 1982;23:577–586.
25. AHA Committee Report. A reporting system on patients evaluated for coronary artery disease. Report of the ad hoc committee for grading of coronary artery disease, council on cardiovascular surgery, American Heart Association. *Circulation* 1975;51(suppl 4):5–40.
26. Bax JJ, Visser FC, van Lingen A, et al. Image quality of cardiac FDG studies in diabetics using hyperinsulinemic glucose clamping [Abstract]. *J Nucl Med* 1995;36:36P/37P.
27. Vom Dahl J, Herman WH, Hicks RJ, et al. Myocardial glucose uptake in patients with insulin-dependent diabetes mellitus assessed quantitatively by dynamic positron emission tomography. *Circulation* 1993;88:395–404.
28. Altehoefer C, Vom Dahl J, Biedermann M, et al. Significance of defect severity in technetium-99m-MIBI SPECT at rest to assess myocardial viability: comparison with fluorine-18-FDG PET. *J Nucl Med* 1994;35:569–574.
29. Hoffman EJ, Huang SC, Phelps ME. Quantitation in positron emission computed tomography: 1. Effect of object size. *J Comp Assist Tomography* 1979;3:299–308.
30. Bonow RO, Dilsizian V, Cuocolo A, Bacharach SL. Identification of viable myocardium in patients with chronic coronary artery disease and left ventricular dysfunction. Comparison of thallium scintigraphy with reinjection and PET imaging with ^{18}F-Fluorodeoxyglucose. *Circulation* 1991;83:26–37.
31. Baer FM, Voth E, Schneider CA, Theissen P, Schicha H, Sechtem U. Comparison of low-dose dobutamine-gradient-echo magnetic resonance imaging and positron emission tomography with [^{18}F]fluorodeoxyglucose in patients with chronic coronary artery disease. A functional and morphological approach to the detection of residual myocardial viability. *Circulation* 1995;91:1006–1015.
32. Soufer R, Dey HM, Lawson AJ, Wackers FJT, Zaret BL. Relationship between reverse redistribution on planar thallium scintigraphy and regional myocardial viability: a correlative PET study. *J Nucl Med* 1995;36:180–187.
33. Sandler MP, Videlefsky S, Delbeke D, et al. Evaluation of myocardial ischemia using a rest metabolism/stress perfusion protocol with fluorine-18-fluorodeoxyglucose/technetium-99m-MIBI and dual-isotope simultaneous-acquisition single-photon emission computed tomography. *J Am Coll Cardiol* 1995;26:864–869.

Matched Ventilation, Perfusion and Chest Radiographic Abnormalities in Acute Pulmonary Embolism

Alexander Gottschalk, Paul D. Stein, Jerald W. Henry and Bruce Relyea
Michigan State University, East Lansing, Michigan and Henry Ford Heart and Vascular Institute, Detroit, Michigan

This investigation assessed the positive predictive value of matched ventilation/perfusion (V/Q) and chest radiographic defects (triple-matched defects) for the detection of acute pulmonary embolism (PE). **Methods:** Data are from the Prospective Investigation of Pulmonary Embolism Diagnosis (PIOPED). Only patients randomized for obligatory pulmonary angiography were included. Lungs were excluded if they showed any mismatched V/Q defect or any pleural effusion. **Results:** Positive predictive values of triple-matched defects in the upper plus middle zones, 1 of 27 (4%), were less frequent than in the lower zones, 13 of 57 (23%) ($p < 0.05$). Triple-matched defects that involved 25–50% of a zone showed PE in 12 of 38 (32%) which was a higher positive predictive value than with smaller or larger triple-matched defects, 2 of 46 (4%) ($p < 0.001$). **Conclusion:** Refinement of the PIOPED data by elimination of nonrandomized patients, elimination of lungs with mismatched perfusion defects and elimination of lungs with a pleural effusion indicate that triple matches with PE (radiographic pulmonary infarcts) are infrequent in the upper and middle lung zones. When a triple match with PE occurs, it is most likely to be 25–50% of a zone.

Key Words: pulmonary embolism; thromboembolism; pulmonary scintiscans; ventilaton/perfusion lung scans

J Nucl Med 1996; 37:1636–1638

The finding of a matched ventilation/perfusion (V/Q) defect with associated matching chest radiographic opacity (the triple match) has been reported to be an intermediate (indeterminate) finding, with a positive predictive value for acute pulmonary

Received July 21, 1995; revision accepted Dec. 13, 1995.
For correspondence or reprints contact: Alexander Gottschalk, MD, Michigan State University, B220 Clin. Science Bldg., East Lansing, MI 48224.